

# Adsorption Properties of Copper (II) Ion from Aqueous Solution by Starch-Grafted Polyacrylamide and Crosslinked Starch-Grafted Polyacrylamide

Jun Tan<sup>1,3</sup> / Xiaoyan Wei<sup>1,3\*</sup> / Yuxia Ouyang<sup>3</sup> / Juhong Fan<sup>2</sup> / Rui Liu<sup>2</sup>

RECEIVED 28 NOVEMBER 2013; ACCEPTED AFTER REVISION 29 APRIL 2014

## Abstract

Starch-grafted polyacrylamide (SA) and cross-linked starch-grafted polyacrylamide (CSA) had been synthesized via grafting polymerization from corn starch and used as adsorbents for the removal of Cu(II) ion from aqueous solution. The equilibrium, kinetics and thermodynamics of adsorption processes of SA and CSA were investigated and compared. It was found that the adsorption capacity of Cu(II) of SA and CSA could reach the maximum within 60 min when the pH was 6. The adsorption kinetics of CSA and SA for Cu(II) was favorably described by the pseudo-second-order kinetic model and the adsorption isotherm was described well with the Freundlich isotherm model. Thermodynamic studies indicated that the adsorption was a spontaneous and endothermic process with increased entropy, and the rise of temperature would benefit the adsorption; the enthalpy change ( $\Delta H$ ), the entropy change ( $\Delta S$ ) and free energy change ( $\Delta G$ ) of the adsorption process of Cu(II) on SA and CSA were calculated with adsorption isotherm data and basic thermodynamic relations.

## Keywords

Adsorption · Copper ion(II) · Starch-grafted polyacrylamide · Cross-linked starch-grafted polyacrylamide · Kinetics · Thermodynamics

## 1 Introduction

The removal of heavy-metal ions from sewage and industrial wastewater has been given lots of attention over the past few years, particularly in China where soil and water have been seriously polluted by heavy metals. Copper is present in wastewaters generated in the electroplating, cement, mining, dyeing and livestock breeding industries. Although copper is an essential trace element, high levels can cause severe environmental and public health problems. The most common adverse health effect of copper in humans is gastrointestinal discomfort. Large amounts of copper can cause hemolysis, liver necrosis and renal injury [1-3]. The US Environmental Protection Agency (US EPA) requires that copper in drinking water doesn't exceed 1.3 mg/L.

Conventional methods for the removal of Cu from wastewater include reduction, ion exchange, evaporation, chemical precipitation and adsorption on activated carbon [4-8]. However, most of these methods have some disadvantages, such as toxic sludge generation and high operation costs when applied for low Cu concentration wastewater on a large scale. This leads to exploration of cheaper and readily available materials for the adsorption of Cu [9,10]. Starch is one of the most abundant natural polymers in the world. Because natural polymers and their derivatives are renewable, biodegradable and capable of adsorbing heavy-metal ions at low cost, some starch derivatives have been widely used for the removal of heavy metal ions. Chan and Wu [11] studied dynamic adsorption behaviors between ion and water-insoluble amphoteric starch in aqueous solutions. Kim & Lim [12] investigated the adsorption of divalent metal ions by cross-linked carboxymethyl corn starch. Guo [13] observed that water-insoluble starch phosphate carbamate had good adsorption performance for Cu(II). Xiang and Li [14] prepared cross-linked amino starch and dithiocarbamate starch and used them for the removal of Cu(II) from aqueous solutions. Dong [15] reported the adsorption behaviors of Cu(II) and Cr(VI) onto amino starch which was synthesized from dialdehyde starch. Nevertheless, these adsorbents have low effective functional groups. In order to solve the problem, high contents of functional groups are needed by graft copolymerization.

<sup>1</sup>Department of Chemical and Textile Engineering of Nanhu College of Jiaxing University, Jiaxing 314001, PR China

<sup>2</sup>Zhejiang Provincial Key Laboratory of Water Science and Technology, Department of Environment, Yangtze Delta Region Institute of Zhejiang, Jiaxing 314006, PR China

<sup>3</sup>College of Biological and Chemical Engineering of Jiaxing University, Jiaxing, 314001, PR China

\*Corresponding author, e-mail: [tanjunzjxu@126.com](mailto:tanjunzjxu@126.com)

Starch-grafted polyacrylamide (SA) is the copolymerization product of starch and acrylamide, which has been widely used in many fields such as papermaking, spinning, petroleum well drilling, medicine, daily chemicals, and floatation [16-18]. Khalil and Farag [19] reported the use of SA as an adsorbent for removing heavy metal cations from aqueous solution. But because of the solubility of SA, the concentration of organic substances in aqueous solution often increased, which was unfavorable for water treatment. Crosslinked starch has infinite molecular mass resulting in its water insolubility; therefore, cross-linked starch-grafted polyacrylamide(CSA) may be reutilized as an adsorbent to remove heavy metal cations from aqueous solution. However, according to our literature survey, few investigations have been made concerning heavy metal cations adsorption onto CSA.

The objective of this study was to investigate the adsorption characteristics of Cu(II) ions from aqueous solution onto CSA. Batch experiments were conducted to compare the Cu(II) adsorption efficiencies for SA and CSA and further investigate the effects of various parameters such as initial solution pH, contact time, initial adsorbate concentration and temperature on the adsorption of Cu(II) onto CSA. The adsorption kinetic data were evaluated by pseudo-first-order and pseudo-second-order models. The adsorption equilibrium data were analyzed by Langmuir and Freundlich isotherm models. Thermodynamic parameters of adsorption such as Gibbs free energy change ( $\Delta G$ ), enthalpy change ( $\Delta H$ ) and entropy change ( $\Delta S$ ) were determined.

## 2 Experiment part

### 2.1 Materials

Corn starch used was food grade (Tianjin DingFeng Factory, China). Epichlorohydrin (EPI), acrylamide (AM), and ceric ammonium nitrate (CAN) (AR, Shanghai Chemical Reagent Factory, Shanghai, China) were used as the cross-linking reagent, graft monomer, and initiator, respectively.  $\text{CuSO}_4$  (AR, Shanghai Chemical Reagent Factory, Shanghai, China) was used in the adsorption experiment. Acetone, sodium chloride, potassium hydroxide, hydrochloric acid and ethanol (AR) were purchased from Hangzhou Chemical Reagent Factory, Hangzhou, China. All aqueous solutions and standards were prepared using deionized water.

### 2.2 Preparation of crosslinked starch (CSt)

CSt was prepared via the following procedure: cornstarch (50 g) and 1% (w/v) sodium chloride solution (75 mL) were added into a 250 mL three-necked flask equipped with a stirrer and a thermometer. The slurry was heated to 30°C in a water bath. Fifteen percentage (w/w) KOH solution (20 mL) was added to the slurry, and then EPI(3.5mL) was added dropwisely for about 5 min. The reaction was kept for 4 h. Upon completion of the reaction, pH values of CSt suspension slurry was

adjusted to 6-7 with 1 mol/L HCl solution. The reaction mixture was washed successively with 250 mL deionized water and 100 mL ethanol, and then filtered by vacuum filtration. Finally, the CSt product was milled and screened after drying in a vacuum oven at 60°C to a constant weight.

### 2.3 Preparation of SA and CSA

Preparation of SA or CSA through graft polymerization was carried out in a three-necked, round-bottom flask. 3.0 g of starch (or CSt) was mixed with 50 mL of distilled water to prepare starch slurry. Then, a known amount of AM (6.0 g) monomer was added to the slurry, and a contact time of 15 min was allowed to facilitate the formation of the emulsion. Subsequently, 10 mL CAN solution ( $6 \text{ mmol} \cdot \text{L}^{-1}$ ) was added to form free radicals on the starch backbone. The volume of the reaction mixture was adjusted to 100 mL by adding distilled water. All the experiments were conducted under a nitrogen atmosphere with constant stirring. The graft polymerization was proceeded at 35°C for 3 h (both the grafting efficiency and the intrinsic viscosity reached the maximum). After the desired reaction period, nitrogen supply was terminated and the graft copolymer was cooled down to room temperature. The solution was precipitated with acetone, thus removing the unreacted monomer. The product was dried at 40°C.

The PAM homopolymer was removed from the precipitated graft copolymer by a Soxhlet extractor with a 40:60 (v/v) mixture of ethylene glycol and acetic acid. The purified SA (or CSA) was then washed with acetone, and was dried in a vacuum oven to a constant weight at 50°C.

The FT-IR spectra of the CSA and SA were analyzed with a NEXUS470 (Nicole Instrument Corporation, USA) using the KBr dispersion method. Compared with the FTIR spectrum of SA, there were no obvious changes in the FTIR spectrum of CSA. From the FTIR spectra of SA and CSA, it was observed that the broad peaks at  $3388 \text{ cm}^{-1}$  were due to the  $-\text{NH}$  stretching vibration of amide group of PAM (overlapped by  $-\text{OH}$  of starch). Smaller peaks at  $2931 \text{ cm}^{-1}$  were assigned to the  $-\text{CH}$  stretching vibrations and peaks at  $931 \text{ cm}^{-1}$ ,  $764 \text{ cm}^{-1}$  and  $704 \text{ cm}^{-1}$  were attributed to carbonyl stretching vibrations of the starch substrate. There were some characteristic absorption peaks occurring at  $1663 \text{ cm}^{-1}$  and  $1593 \text{ cm}^{-1}$  which correspond to  $-\text{C}=\text{O}$  and  $-\text{C}=\text{O}$  (hydrogen bonded) stretching vibration of the  $-\text{CONH}_2$  groups, and the peaks at  $1153 \text{ cm}^{-1}$  were due to C-N stretching. The presence of these additional peaks in grafted starch compared to that of non-grafted starch confirms the successful grafting of PAM chains onto the backbone of starch or the crosslinked starch.

The  $\text{pH}_{\text{pzc}}$  values of SA and CSA measured were 5.75 and 5.81, respectively. The importance of  $\text{pH}_{\text{pzc}}$  value is that it is expected that the removal of Cu(II) ion would be feasible below this pH at which the absorbents' surface would have a net positive charge.

Elemental analysis studies of dry samples were performed on a Flash EA-1112 elemental analyzer (Thermo Finnigan Corporation, Italy). The results showed that SA contained 9.86% nitrogen, 44.32% carbon, and 7.31% hydrogen, while CSA contained 10.71% nitrogen, 44.01% carbon, and 7.35% hydrogen, respectively.

The intrinsic viscosity of the graft copolymers were determined with an Ubbelohde viscometer at  $30 \pm 0.1^\circ\text{C}$  in 1 M aqueous NaCl solution [20]. The intrinsic viscosity values of SA and CSA were 238 mL/g and 413 mL/g, respectively.

## 2.4 Adsorption experiment

The adsorption experiments were carried out in a series of 200 mL Erlenmeyer flasks containing a certain amount of CSA (or SA) and 100 mL of  $\text{CuSO}_4$  solutions with known  $\text{Cu}^{2+}$  concentrations and initial pH (adjusted with 0.1 N hydrochloric acid or 0.1 N NaOH). The mixtures were then shaken at 150 rpm in a thermostatic water-bath shaker at 288 K. After shaking for a certain period of time, the supernatant was removed from the flask and the concentration of  $\text{Cu}^{2+}$  in the aqueous phase was analyzed. All results were performed in triplicate, and the data were recorded as means. The adsorption capacity of SA (or CSA) was calculated with Eq. (1):

$$Q = \frac{(C_0 - C_t)V}{W} \quad (1)$$

where,  $Q$  is the adsorption capacity of Cu(II) on SA (or CSA) (mg/g);  $C_0$  and  $C_t$  (mg/L) are the initial concentrations of Cu(II) ions and Cu(II) concentrations at time  $t$ , respectively;  $V$  is the total volume of the aqueous solution (L); and  $W$  is the dose weight of SA (or CSA) (g).

The concentrations of Cu(II) in the aqueous solutions were measured using an atomic absorption spectrophotometer (AA800 spectrometer, PerkinElmer, USA).

## 3 Results and discussion

### 3.1 Effect of pH on the adsorption process

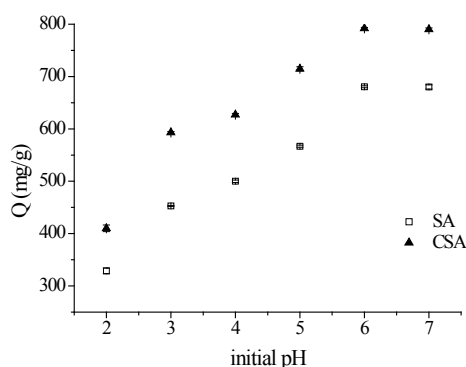


Fig. 1. Effect of initial pH of the solution on adsorption capacity ( $\text{Cu}^{2+} = 30 \text{ mg/L}$ ;  $T = 288\text{K}$ ; contacted time = 3 h; the adsorbent dosage = 30 mg/L)

The influence of the initial pH on the adsorption of  $\text{Cu}^{2+}$  onto SA and CSA was examined in the pH range of 2.0–7.0 (Fig. 1). It can be seen from Fig.1 that  $Q$  increased significantly with the increase of pH from 2.0 to 6.0, and then the increase slowed is slowing down as pH exceeded 6.0. As pH was higher than 7.0, the precipitation of  $\text{Cu}^{2+}$  ions took place.

The influence of the solution pH on the metal ions uptake can be explained on the basis of the  $\text{pH}_{\text{PZC}}$  of the adsorbent [21]. Because the  $\text{pH}_{\text{PZC}}$  of SA and CSA was 5.75 and 5.81, respectively, when pHs of solutions were lower than  $\text{pH}_{\text{PZC}}$  of SA and CSA, the surface of the adsorbents was positively charged, and a high concentration of  $\text{H}^+$  ions competed with  $\text{Cu}^{2+}$  on the surface of adsorbents, which hindered the adsorption of  $\text{Cu}^{2+}$  on the adsorbent surface. As pH value increased, the competitive adsorption of  $\text{H}^+$  ions decreased [22], and the capacity adsorption of  $\text{Cu}^{2+}$  was improved rapidly. When pH was higher than  $\text{pH}_{\text{PZC}}$ , the negative charge density on the adsorbents surface was favorable for the adsorption of  $\text{Cu}^{2+}$  ions through electrostatic interaction and surface complexation.

Both adsorbents had the same trends. The higher capacity of  $\text{Cu}^{2+}$  ions on CSA (792 mg/g) than that of SA (680.5 mg/g), may be attributed to the higher content of nitrogen of CSA, which means CSA contained more amide groups ( functional groups).

### 3.2 Effect of adsorption time

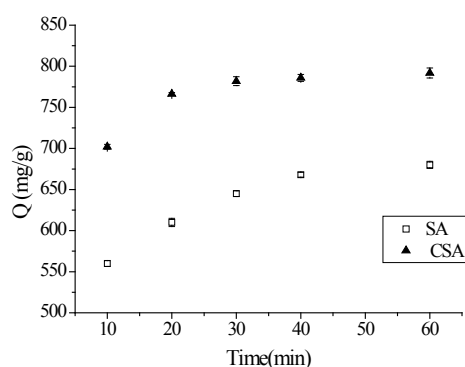


Fig. 2. Effect of adsorption time on adsorption ( $\text{Cu}^{2+} = 30 \text{ mg/L}$ ;  $T = 288\text{K}$ ;  $\text{pH} = 6$ ; the adsorbent dosage = 30 mg/L)

The  $\text{Cu}^{2+}$  adsorption capacity of SA and CSA was compared as a function of adsorption time. As shown in Fig. 2, the removal of  $\text{Cu}^{2+}$  by the two adsorbents was increased with the increase in the adsorption time and the adsorption rate was initially rapid, and over 70% of the adsorption was completed within 10 min and the adsorption equilibrium was attained in 60 min. The adsorption rate of  $\text{Cu}^{2+}$  ions was fast due to a large number of vacant active groups on the adsorbents available for adsorption at the beginning, but became slower near the equilibrium due to quick exhaustion of the adsorption sites and the repulsive forces between  $\text{Cu}^{2+}$  adsorbed on the solid adsorbents

and in the aqueous phases. This result indicates that  $\text{Cu}^{2+}$  ions can rapidly form chelates with the amide groups of starch. The rapid interaction of metal ions with starch would be beneficial for practical use. The result also indicates that the equilibrium time for SA and CSA was almost 60 min. For the subsequent experiments, the treatment time was maintained at 60 min to ensure that the adsorption equilibrium was achieved.

### 3.3 Adsorption kinetics study

Adsorption kinetics and equilibria are important for the evaluation of the basic traits of a good adsorbent [23]. To investigate adsorption kinetics of  $\text{Cu}^{2+}$  on SA and CSA, both pseudo-first-order and pseudo-second-order kinetic models were used to identify the rate and kinetics of the adsorption of  $\text{Cu}^{2+}$  ions.

The linear form of the pseudo-first-order equation [24, 25] is given by:

$$\ln(Q_e - Q_t) = \ln Q_e - k_1 t \quad (2)$$

where,  $Q_t$  and  $Q_e$  (all in mg/g) are the adsorption amounts of  $\text{Cu}^{2+}$  in aqueous solutions at equilibrium and at any time  $t$ , respectively.  $k_1$  is the rate constant of the pseudo-first-order adsorption. The values of  $Q_e$  (calculated),  $k_1$  and the correlation coefficients were determined from the linear plot of  $\ln(Q_e - Q_t)$  versus  $t$  (Fig.3(a)) and are shown in Table 1.

The linear pseudo-second-order equation [26, 27] is given by:

$$\frac{t}{Q_t} = \frac{1}{k_2 Q_e^2} + \frac{t}{Q_e} \quad (3)$$

where  $k_2$  is the rate constant of the pseudo-second-order kinetics. The plot of  $t/Q_t$  versus  $t$  for the adsorption of  $\text{Cu}^{2+}$  was plotted and is shown in Fig. 3(b). From the slope and intercept values, the values of  $Q_e$  (cal.) and  $k_2$  were calculated and are shown in Table 1.

It is clear from the results that the theoretical  $Q_e$  (cal.) values more agree with the experimental ones  $Q_e$  (exp.) obtained from the pseudo-second-order kinetics. Furthermore, all the correlation coefficients ( $R^2$ ) for the pseudo-second-order kinetic model are more than 0.99 (0.99965 and 0.9999 for SA and CSA, respectively), implying that the adsorption of  $\text{Cu}(\text{II})$  ions can be described more favorably by pseudo-second-order process. A similar observation was reported on the adsorption of  $\text{Cu}^{2+}$  from aqueous solution using adsorbents with active groups [13, 15, 28].

From experimental data adsorption rate constants for SA and CSA were calculated and are shown in Table 1. It can be seen that the adsorption rate and capacity of CSA was higher than that of SA. This may be attributed to the fact that the crosslinked starch graft copolymer with a higher grafting percentage has more amide groups, which would increase the adsorption ability toward  $\text{Cu}(\text{II})$  ions due to stronger complexation.

### 3.4 Effect of initial concentration of $\text{Cu}^{2+}$ ion on adsorption capacity

The effect of initial  $\text{Cu}(\text{II})$  concentration on the adsorption capacities on SA and CSA were investigated by varying the initial concentration from 30 to 180 mg/L. As shown

Tab. 1. Pseudo-first-order and pseudo-second-order model parameters for the adsorption of  $\text{Cu}^{2+}$  ions on SA and CSA

Sample	$Q_e$ (exp.) (mg/ g)	Pseudo-first-order			Pseudo-second-order		
		$Q_e$ (cal.) ( mg/ g)	$k_1$ (1/min)	$R^2$	$Q_e$ (cal.) (mg/ g)	$k_2$ (g/ mg·min)	$R^2$
SA	680.5	608.2	0.11002	0.9293	714.0	0.328	0.99965
CSA	792.0	702.2	0.12515	0.9416	813.0	0.783	0.9999

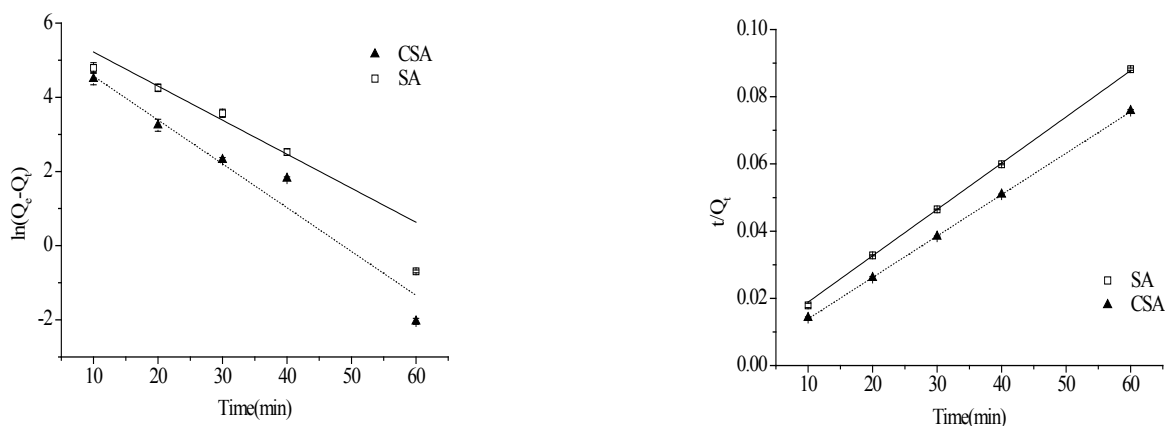


Fig. 3. Pseudo-first-order (a) and pseudo-second-order (b) kinetic model plots ( $\text{Cu}^{2+} = 30$  mg/L;  $T = 288\text{K}$ ;  $\text{pH} = 6$ ; the adsorbent dosage = 30 mg/L)

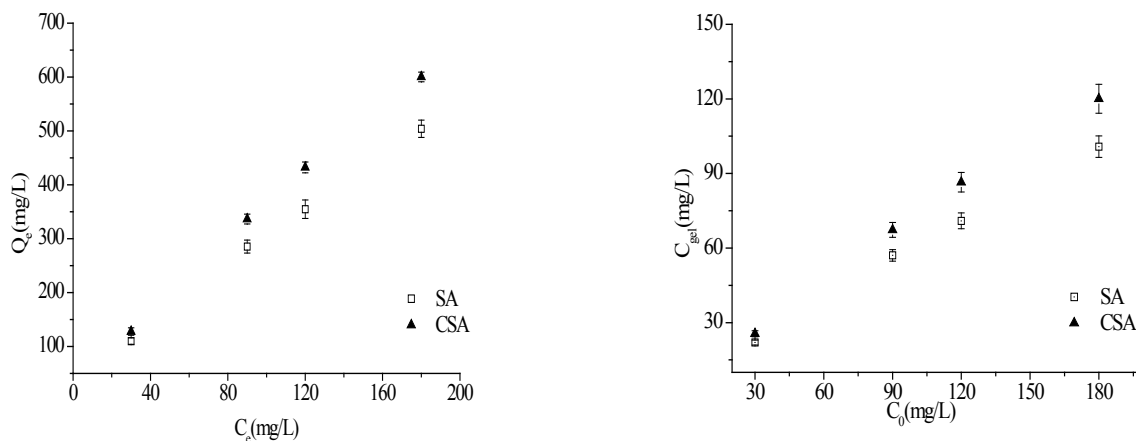
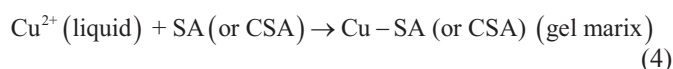


Fig. 4. Effect of initial concentration of copper ions (a) on adsorption capacity and (b) the concentration of copper ions in the gel matrix ( $T = 288K$ ;  $pH = 6$ ; contacted time = 60min; the highest absorbent dosage = 200mg/L)

in Fig. 4, the adsorption capacities of SA and CSA increased significantly with increasing the initial  $Cu(II)$  concentration;  $Q$  of SA and CSA increased from 109.95 to 503.95 mg/g, and 127.68 to 600.3 mg/g, respectively, while the concentrations of copper ions in the gel matrix ( $C_{gel}$ ) increased from 21.99 to 100.79mg/L, and 25.45 to 120.06 mg/L, respectively. The reason for the increase can be explained using the adsorption reactions described as follows:



Eq. (4) shows that the increase of  $Cu^{2+}$  concentration can shift the reaction to the right and cause higher adsorption. In Tab. 2, the partition coefficients decreased with increasing the initial  $Cu(II)$  concentration, which resulted from the initial  $Cu(II)$  concentration increasing faster than ions that were adsorbed on the surface of the adsorbents. The increase in the adsorption capacity on CSA was much higher than SA due to more amide groups, resulting in significant adsorption differences at high copper ion concentrations.

Tab. 2. The partition coefficients of copper ions ( $K$ ) on SA and CSA at different initial  $Cu(II)$  concentration

$C_0$ (mg/L)	30	90	120	180
$K_{SA}$	2.745	1.732	1.446	1.272
$K_{CSA}$	5.726	2.964	2.579	2.003

( $K$  is equal to the ratio of the concentration of copper ions in the gel matrix and in the solution after reaching the adsorption equilibrium)

### 3.5 Adsorption isotherm

The adsorption equilibrium data obtained at various initial  $Cu^{2+}$  concentrations were used to assess the adsorption isotherm with the two popular adsorption models: Langmuir and

Freundlich isotherm. Langmuir adsorption isotherm models the monolayer coverage on the adsorption surface. It assumes that adsorption occurs at specific homogeneous adsorption sites on the adsorbent surface and intermolecular forces decrease rapidly with the distance from the adsorption surface. The Langmuir adsorption model further assumes that all the adsorption sites are energetically identical and adsorption occurs on a structurally homogeneous adsorbent. The Langmuir isotherm equation [29] can be expressed in Eq. (5):

$$\frac{C_e}{Q_e} = \frac{1}{Q_m b} + \frac{C_e}{Q_m} \quad (5)$$

where  $C_e$  is the equilibrium concentration of  $Cu^{2+}$  in aqueous solutions (mg/L),  $Q_e$  is the adsorption amount of  $Cu^{2+}$  in aqueous solutions at equilibrium (mg/g),  $Q_m$  is the maximum adsorption amount of  $Cu^{2+}$  in aqueous solutions at equilibrium (mg/g), and  $b$  is the Langmuir constant (L/mg).

Freundlich adsorption isotherm equation [30] is derived to model the multilayer adsorption on heterogeneous surfaces and can be described by Eq (6):

$$\lg Q_e = \lg K_f + \frac{1}{n} \lg C_e \quad (6)$$

where  $K_f$  is the Freundlich constant which is related to the adsorption capacity of the adsorbent, and  $1/n$  is the Freundlich constant related to adsorption intensity.

The values of  $Q_m$  and  $b$  were calculated from the slope and the intercept of the linear plot of  $C_e/Q_e$  versus  $C_e$  (Fig. 5a) and the values of  $K_f$  and  $n$  were calculated from the slope and the intercept of the linear plot between  $\lg Q_e$  and  $\lg C_e$  (Fig. 5b). The values are presented in Tab. 3.

The  $R^2$  values for the Freundlich isotherms for the adsorption of  $Cu^{2+}$  on SA and CSA were above 0.99 (Table 3), indicating that adsorption of  $Cu^{2+}$  on the two adsorbents can be better described with the Freundlich isotherm. This observation

Tab. 3. Langmuir and Freundlich parameters for the adsorption of Cu<sup>2+</sup> ions on SA and CSA

Sample	Langmuir			Freundlich		
	Q <sub>m</sub> (mg/g)	b(L/mg)	R <sup>2</sup>	K <sub>f</sub> (mg/g)	n	R <sup>2</sup>
SA	847.46	0.0166	0.91262	52.48	1.52	0.99869
CSA	877.19	0.0319	0.93232	27.91	1.67	0.99974

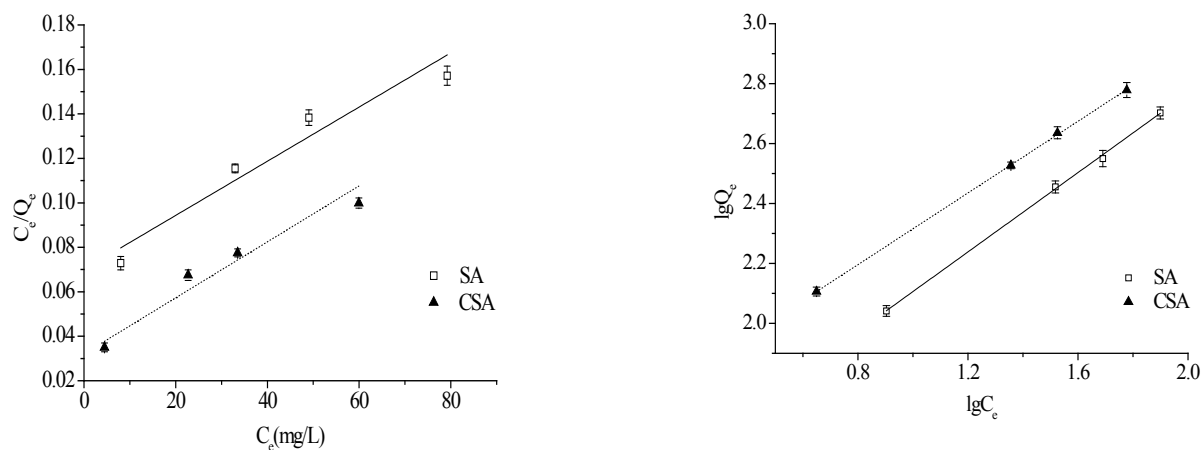


Fig. 5. Langmuir (a) and Freundlich (b) adsorption isotherms of Cu<sup>2+</sup> ions on SA and CSA (T = 288K; pH = 6; contacted time = 60 min; the adsorbent dosage = 200 mg/L)

suggests that the two adsorbents' surfaces which could adsorb copper ion were heterogeneous. Perhaps the amide groups and the -OH groups resided on starch chains along with the porous structure of the starch granule all contributed to absorption of Cu<sup>2+</sup> ions, therefore the physical absorption of Cu<sup>2+</sup> ions could be an additional mechanism for metal removal by SA or CSA.

### 3.6 Thermodynamics of the adsorption

The thermodynamics for adsorption of Cu<sup>2+</sup> ion on SA and CSA were determined at different temperatures. It is found that the adsorption capacities were increased with the increase in temperature, showing the endothermic nature of the adsorption with the temperature in the range of 283 to 303 K.

Thermodynamic parameters [31, 32], such as free energy change ( $\Delta G$ ), enthalpy change ( $\Delta H$ ) and entropy change ( $\Delta S$ ), were estimated using the following equations.  $D$  represents the distribution coefficient (L/g), which is equal to the absorption equilibrium constant at the solid/liquid phase, and is shown as a function of the temperature. Because the relationship between  $\lg D$  and  $1/T$  for SA and CSA is linear, the changes in the adsorption enthalpy ( $\Delta H$ ) and entropy ( $\Delta S$ ) can be calculated with the Van't Hoff equation (8):

$$D = \frac{Q_e}{C_e} \quad (7)$$

$$\lg D = -\Delta H / (2.303RT) + \Delta S / R \quad (8)$$

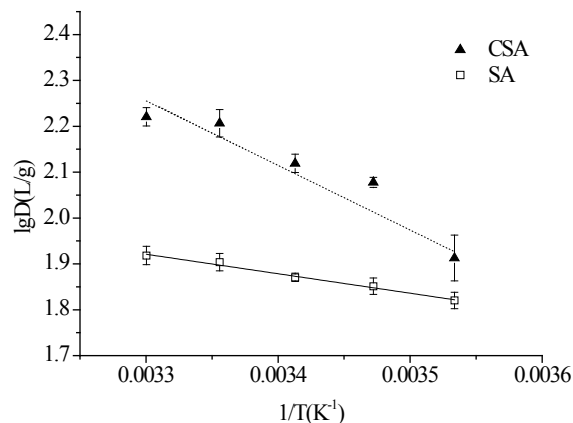


Fig. 6. Plots of  $\lg D$  versus  $1/T$  for the adsorption of Cu(II) on SA and CSA (Cu<sup>2+</sup> = 30 mg/L; pH = 6; contacted time = 60 min; the adsorbent dosage = 30 mg/L)

where,  $R$  is the gas constant ( $J/mol \cdot K$ ) and  $T$  is the temperature ( $K$ ). The plots of  $\lg D$  against  $1/T$  for Cu<sup>2+</sup> ions are shown in Fig. 6. The values of  $\Delta H$  and  $\Delta S$  were obtained from the slope and intercept of  $\lg D$  vs  $1/T$  plots, which were calculated by a curve-fitting program. Gibbs free energy ( $\Delta G$ ) was calculated with the following thermodynamic equation:

$$\Delta G = \Delta H - T\Delta S \quad (9)$$

where,  $D$  is the distribution coefficient (L/g) and  $R$  is the gas constant ( $J/mol \cdot K$ ). According to Eq. (8), the values of  $\Delta H$  and  $\Delta S$  can be calculated from the slopes ( $\Delta H/2.303R$ ) and intercepts ( $\Delta S/R$ ) of the plots of  $\lg D$  versus  $1/T$ .  $\Delta G$  was calculated

Tab. 4. Thermodynamic parameters for the adsorption of Cu<sup>2+</sup> on SA and CSA

Sample	T (K)	Q <sub>e</sub> (mg/g)	D (L/g)	ΔG (kJ/mol)	ΔH (kJ/mol)	ΔS (J/mol•K)
SA	283	664.80	66.10979	-9.87508	8.169	63.760
	288	680.53	71.00723	-10.1939		
	293	690.13	74.23982	-10.5127		
	298	706.27	80.14828	-10.8315		
	303	713.07	82.83767	-11.1503		
CSA	283	710.53	81.82097	-10.5118	24.583	124.301
	288	792.00	119.5719	-11.1319		
	293	797.87	131.5743	-11.7519		
	298	828.40	160.9169	-12.372		
	303	832.93	166.1878	-12.992		

from the thermodynamic equation (9). The calculated values of the thermodynamic parameters are given in Tab. 4.

As it can be seen from Tab. 4, the ΔH values are found to be positive for all cases revealing that the adsorption processes were endothermic in nature. Negative values of ΔG indicate the adsorption processes were spontaneous and thermodynamically favorable. The values of ΔG became more negative with the increase in temperature, indicating that the adsorption processes would be more favorable at high temperature. The similar results are found in the studies of Wang and Qin [33], Rakhshaei et al. [34], Xie et al. [35] and Yin et al. [36]. The positive values of ΔS showed the affinity of SA or CSA for Cu<sup>2+</sup> ions increased the disorder at the solid/liquid interface during the adsorption process. Generally, the change in free energy for physical adsorption is between -20 kJ/mol and 0, and that for chemical adsorption is between -80 and -400 kJ/mol [37]. The values of ΔG obtained in this study are in the range of physical adsorption, suggesting that the adsorption of Cu<sup>2+</sup> onto SA or CSA are both physical adsorption.

## 4 Conclusions

CSA exhibited higher adsorption capacity for Cu(II) ions than SA. Various factors including solution pH, contact time, initial Cu(II) concentration and temperature were studied. The results showed the adsorption capacity of Cu(II) on CSA increased with the increase of solution pH from 2 to 6. The adsorption kinetic process was well predicted by the pseudo-second-order kinetic model and the adsorption equilibrium data were correlated well with the Freundlich isotherm model. Based on the Freundlich isotherm model, the maximum Cu(II) adsorption capacity for CSA at pH=6 was 792 mg/g. The negative value of ΔG showed that the adsorption of Cu(II) onto CSA was a spontaneous and physical adsorption process. The positive value of ΔH showed the endothermic nature of adsorption. The positive values of ΔS showed the affinity of CSA for Cu(II) ions increased the disorder at the solid/liquid interface during the adsorption process. Results of this study suggest that CSA is a promising adsorbent for the removal of Cu(II) ions from aqueous solution.

## Acknowledgement

This work was financially supported by the Hi-Tech Research and Development Program of China (NO.2012AA06A304), the Research Project for Application of Public Technology of Zhejiang Province (NO.2012C31028), the Platform funds from Zhejiang Province (NO.2012F10028), the Science and Technology Project Foundation of Jiaxing City, P. R. China (2012AY1025) and the research funds from Nanhu College of Jiaxing University (NO.N41472001-3).

## References

- Sheng P. X., Ting Y. P., Chen J. P., Hong L., *Sorption of lead, copper, cadmium, zinc, and nickel by marine algal biomass: characterization of biosorptive capacity and investigation of mechanisms*. Journal of Colloid Interface Science, 275 (1), pp. 131-141, (2004). DOI: [10.1016/j.jcis.2004.01.036](https://doi.org/10.1016/j.jcis.2004.01.036)
- Wan Ngah W. S., Hanafiah M. A. K. M., *Removal of heavy metal ions from wastewater by chemically modified plant wastes as adsorbents: A review*. Bioresource Technology, 99 (10), pp. 3935-3948, (2008). DOI: [10.1016/j.biortech.2007.06.011](https://doi.org/10.1016/j.biortech.2007.06.011)
- Kurniawan T. A., Chan G. Y. S., Lo W. H., Babel S., *Comparisons of low-cost adsorbents for treating wastewaters laden with heavy metals*. Science of The Total Environment, 366 (2-3), pp. 409-426, (2006). DOI: [10.1016/j.scitotenv.2005.10.001](https://doi.org/10.1016/j.scitotenv.2005.10.001)
- Fu F. L., Wang Q., *Removal of heavy metal ions from wastewaters: A review*. Journal of Environment Management, 92 (3), pp. 407-418, (2011). DOI: [10.1016/j.jenvman.2010.11.011](https://doi.org/10.1016/j.jenvman.2010.11.011)

- 5 **Amarasinghe B. M. W. P. K., Williams R. A.,** *Tea waste as a low cost adsorbent for the removal of Cu and Pb from wastewater.* Chemical Engineering Journal, 132 (1-3), pp. 299-309, (2007). DOI: [10.1016/j.cej.2007.01.016](https://doi.org/10.1016/j.cej.2007.01.016)
- 6 **Ahmady-Asbchin S., Andres Y., Gerente C., Le Cloirec P.,** *Biosorption of Cu(II) from aqueous solution by Fucus serratus: Surface characterization and sorption mechanisms.* Bioresource Technology, 99 (14), pp. 6150-6155, (2008). DOI: [10.1016/j.biortech.2007.12.040](https://doi.org/10.1016/j.biortech.2007.12.040)
- 7 **Nuhoglu Y., Malkoc E., Gürses A., Canpolat N.,** *The removal of Cu(II) from aqueous solutions by Ulothrix zonata.* Bioresource Technology, 85 (3), pp. 331-333, (2002). DOI: [10.1016/S0960-8524\(02\)00098-6](https://doi.org/10.1016/S0960-8524(02)00098-6)
- 8 **Sengil I. A., Özacar M.,** *Biosorption of Cu(II) from aqueous solutions by mimosa tannin gel.* Journal of Hazardous Materials, 157 (2-3), pp. 277-285, (2008). DOI: [10.1016/j.jhazmat.2007.12.115](https://doi.org/10.1016/j.jhazmat.2007.12.115)
- 9 **Babel S., Kurniawan T. A.,** *Low-cost adsorbents for heavy metals uptake from contaminated water: a review.* Journal of Hazardous Materials, 97 (1-3), pp. 219-243, (2003). DOI: [10.1016/S0304-3894\(02\)00263-7](https://doi.org/10.1016/S0304-3894(02)00263-7)
- 10 **Crini G.,** *Recent developments in polysaccharide-based materials used as adsorbents in wastewater treatment.* Progress in Polymer Science, 30 (1), pp. 38-70, (2005). DOI: [10.1016/j.progpolymsci.2004.11.002](https://doi.org/10.1016/j.progpolymsci.2004.11.002)
- 11 **Chan W. C., Wu J. Y.,** *Dynamic adsorption behaviors between Cu<sup>2+</sup> ion and water-insoluble amphoteric starch in aqueous solutions.* Journal of Applied Polymer Science, 81 (12), pp. 2849-2855, (2001). DOI: [10.1002/app.1734](https://doi.org/10.1002/app.1734)
- 12 **Kim B. S., Lim S.-T.,** *Removal of heavy metal ions from water by cross-linked carboxymethyl corn starch.* Carbohydrate Polymers, 39 (3), pp. 217-223, (1999). DOI: [10.1016/S0144-8617\(99\)00011-9](https://doi.org/10.1016/S0144-8617(99)00011-9)
- 13 **Guo L., Zhang S. F., Ju B. Z., Yang J. Z.,** *Study on adsorption of Cu(II) by water-insoluble starch phosphate carbamate.* Carbohydrate Polymers, 63 (4), pp. 487-492, (2006). DOI: [10.1016/j.carbpol.2005.10.006](https://doi.org/10.1016/j.carbpol.2005.10.006)
- 14 **Li Y. J., Xiang B., Ni Y. M.,** *Removal of Cu(II) from aqueous solutions by chelating starch derivatives.* Journal of Applied Polymer Science, 92 (6), pp. 3881-3885, (2004). DOI: [10.1002/app.20415](https://doi.org/10.1002/app.20415)
- 15 **Dong A. Q., Xie J., Wang W. M., Yu L. P., Liu Q. A., Yin Y. P.,** *A novel method for amino starch preparation and its adsorption for Cu(II) and Cr(VI).* Journal of Hazardous Materials, 181 (1-3), pp. 448-454, (2010). DOI: [10.1016/j.jhazmat.2010.05.031](https://doi.org/10.1016/j.jhazmat.2010.05.031)
- 16 **Sen G., Kumar R., Ghosh S., Pal S.,** *A novel polymeric flocculant based on polyacrylamide grafted carboxymethylstarch.* Carbohydrate Polymers, 77 (4), pp. 822-831, (2009). DOI: [10.1016/j.carbpol.2009.03.007](https://doi.org/10.1016/j.carbpol.2009.03.007)
- 17 **Bratskaya S., Schwarz S., Liebert T., Heinze T.,** *Starch derivatives of high degree of functionalization 10. Flocculation of kaolin dispersions.* Colloids and Surfaces A: Physicochemical and Engineering Aspects, 254 (1-3), pp. 75-80, (2005). DOI: [10.1016/j.colsurfa.2004.11.030](https://doi.org/10.1016/j.colsurfa.2004.11.030)
- 18 **Mishra S., Mukul A., Sen G., Jha U.,** *Microwave assisted synthesis of polyacrylamide grafted starch (St-g-PAM) and its applicability as flocculant for water treatment.* International Journal of Biological Macromolecules, 48 (1), pp. 106-111, (2011). DOI: [10.1016/j.ijbiomac.2010.10.004](https://doi.org/10.1016/j.ijbiomac.2010.10.004)
- 19 **Khalil M. I., Farag S.,** *Utilization of some starch derivatives in heavy metal ions removal.* Journal of Applied Polymer Science, 69 (1), pp. 45-50, (1998). DOI: [10.1002/\(SICI\)1097-4628\(19980705\)69:1<45::AID-APP6>3.0.CO;2-M](https://doi.org/10.1002/(SICI)1097-4628(19980705)69:1<45::AID-APP6>3.0.CO;2-M)
- 20 **Collins E. A., Bares J., Billmeyer F. W.,** *Experiments in Polymer Science,* John Wiley & Sons, New York, pp. 394-399 (1973).
- 21 **Fan L., Chen Y., Wang L., Jiang W. J.,** *Adsorption of Pb(II) Ions from Aqueous Solutions by Pyrolusite-modified Activated Carbon Prepared from Sewage Sludge.* Adsorption Science and Technology, 29 (5), pp. 495-506, (2011). DOI: [10.1260/0263-6174.29.5.495](https://doi.org/10.1260/0263-6174.29.5.495)
- 22 **Sreejalekshmi K. G., Krishnan K. A., Anirudhan T. S.,** *Adsorption of Pb(II) and Pb(II)-citric acid on sawdust activated carbon: Kinetic and equilibrium isotherm studied.* Journal of Hazardous Materials, 161 (2-3), pp. 1506-1513, (2009). DOI: [10.1016/j.jhazmat.2008.05.002](https://doi.org/10.1016/j.jhazmat.2008.05.002)
- 23 **Wang X. J., Chen L., Xia S. Q., Zhao J., Chovelon J.-M., Renault J. N.,** *Biosorption of Cu(II) and Pb(II) from aqueous solutions by dried activated sludge.* Minerals Engineering, 19 (9), pp. 968-971, (2006). DOI: [10.1016/j.mineng.2005.09.042](https://doi.org/10.1016/j.mineng.2005.09.042)
- 24a **Ho Y. S., McKay G.,** *The kinetics of sorption of divalent metal ions onto sphagnum moss peat.* Water Resource, 34 (3), pp. 735-742, (2000). DOI: [10.1016/S0043-1354\(99\)00232-8](https://doi.org/10.1016/S0043-1354(99)00232-8)
- 24b **Ho Y. S.,** *Review of second-order models for adsorption system.* Journal of Hazardous Materials, 136 (3), pp. 681-689, (2006). DOI: [10.1016/j.jhazmat.2005.12.043](https://doi.org/10.1016/j.jhazmat.2005.12.043)
- 25 **Langmuir I.,** *The Adsorption of Gases on Plane Surfaces of Glass, Mica and Platinum.* Journal of the American Chemical Society, 40 (9), pp. 1361-1403, (1918). DOI: [10.1021/ja02242a004](https://doi.org/10.1021/ja02242a004)
- 26 **Freundlich H.,** *Concerning adsorption in solutions.* Z Phys Chem-Stoch Ve, 57, pp. 385-470, (1906).
- 27 **Reddy M. R., Dunn S. J.,** *Distribution Coefficients for Nickel and Zinc in Soils.* Environmental Pollution Series B, Chemical and Physical, 11 (4), pp. 303-313, (1986).
- 28 **Guo L., Li G. Y., Liu J. S., Meng Y. F., Tang Y. F.,** *Adsorptive decolorization of methylene blue by crosslinked porous starch.* Carbohydrate Polymers, 93 (2), pp. 374-379, (2013). DOI: [10.1016/j.carbpol.2012.12.019](https://doi.org/10.1016/j.carbpol.2012.12.019)
- 29 **Denizli A., Salih B., Piskin E.,** *New sorbents for removal of heavy metal ions: Diamine-glow-discharge treated polyhydroxyethylmethacrylate microspheres.* Journal of Chromatography A, 773 (1-2), pp. 169-178, (1997). DOI: [10.1016/S0021-9673\(97\)00187-8](https://doi.org/10.1016/S0021-9673(97)00187-8)
- 30 **Ucer A., Uyanik A., Aygun S. F.,** *Adsorption of Cu(II), Cd(II), Zn(II), Mn(II) and Fe(III) ions by tannic acid immobilised activated carbon.* Separation and Purification Technology, 47 (3), pp. 113-118, (2006). DOI: [10.1016/j.seppur.2005.06.012](https://doi.org/10.1016/j.seppur.2005.06.012)
- 31 **Unlu N., Ersoz M.,** *Adsorption characteristics of heavy metal ions onto a low cost biopolymeric sorbent from aqueous solutions.* Journal of Hazardous Materials, 136 (2), pp. 272-280, (2006). DOI: [10.1016/j.jhazmat.2005.12.013](https://doi.org/10.1016/j.jhazmat.2005.12.013)
- 32 **Donat R., Akdogan A., Erdem E., Cetisli H.,** *Thermodynamics of Pb<sup>2+</sup> and Ni<sup>2+</sup> adsorption onto natural bentonite from aqueous solutions.* Journal of Colloid and Interface Science, 286 (1), pp. 43-52, (2005). DOI: [10.1016/j.jcis.2005.01.045](https://doi.org/10.1016/j.jcis.2005.01.045)

- 33 Xie G., Shang X., Liu R., *Synthesis and characterization of a novel amino modified starch and its adsorption properties for Cd(II) ions from aqueous solution*. Carbohydrate Polymers, 84 (1), pp. 430-438, (2011).  
DOI: [10.1016/j.carbpol.2010.12.003](https://doi.org/10.1016/j.carbpol.2010.12.003)
- 34 Wang X. S., Qin Y., *Removal of Ni(II), Zn(II) and Cr(VI) from aqueous solution by Alternanthera philoxeroides biomass*. Journal of Hazardous Materials, 138 (3), pp. 582-588, (2006).  
DOI: [10.1016/j.jhazmat.2006.05.091](https://doi.org/10.1016/j.jhazmat.2006.05.091)
- 35 Rakhshae R., Khosravi M., Ganji M. T., *Kinetic modeling and thermodynamic study to remove Pb(II), Cd(II), Ni(II) and Zn(II) from aqueous solution using dead and living Azolla filiculoides*. Journal of Hazardous Materials, 134 (1-3), pp. 120-129, (2006).  
DOI: [10.1016/j.jhazmat.2005.10.042](https://doi.org/10.1016/j.jhazmat.2005.10.042)
- 36 Chen H., Dai G. L., Zhao J., Zhong A. G., Wu J. Y., Yan H., *Removal of copper(II) ions by a biosorbent-Cinnamomum camphora leaves powder*. Journal of Hazardous Materials, 177 (1-3), pp. 228-236, (2010).  
DOI: [10.1016/j.jhazmat.2009.12.022](https://doi.org/10.1016/j.jhazmat.2009.12.022)